UDK 621.7.016.5:621.315.612:621.694
Original scientific article/Izvirni znanstveni članek

ISSN 1580-2949
MTAEC9, 53(6)777(2019)

PIERCING BEHAVIOR OF AN *IN-SITU* C_f/Al_2O_3 COMPOSITE IN WATERJET MACHINING

IN-SITU MEHANSKA OBDELAVA C_f/Al_2O_3 KOMPOZITA Z VODNIM CURKOM

Jie Ren[1,2], Xu Qiao[3*]

[1]Editorial Office of Journal of the Chinese Ceramic Society, The Chinese Ceramic Society, Beijing 100831, China
[2]Department of Materials Science and Engineering, China University of Mining and Technology, Beijing 100083, China
[3]Department of Computer Science, China University of Mining and Technology, Beijing 100083, China

Prejem rokopisa – received: 2019-03-26; sprejem za objavo – accepted for publication: 2019-05-17

doi:10.17222/mit.2019.066

Short fiber/ceramic composites with a relatively low price and facile preparation procedure have been widely used, and waterjet is commonly used to machine hard materials because of its high efficiency. However, there is a limited number of works on the waterjet-machining behavior of ceramic incorporated with short fibers. In this study, an in-situ C_f/Al_2O_3 composite was prepared by in-situ transforming pre-oxidized poly-acrylonitrile fibers into carbon fibers during uni-axial hot-pressed sintering of an alumina matrix. Under the uni-axial pressure, the fibers were preferably orientated parallel to the hot-pressed surface. Pristine Al_2O_3 ceramic was selected to be compared with the composite. Experimental results demonstrated that the machined surface with most of its fibers being parallel to it exhibited a satisfactory machining behavior. In this situation, the average piercing depth of the composite was approximately 1.5 and 5–7 times higher than that of the Al_2O_3 ceramic machined with pure waterjet and abrasive waterjet, respectively. Erosion mechanisms associated with the pure-waterjet piercing of the composite were alumina-matrix intergranular or transgranular fractures and fiber spalling or fracture. For the abrasive waterjet, micro-fracture of the alumina grains and fibers together with a grain plastic deformation and abrasive micro-melting were discovered to be the dominant erosion mechanisms. It was concluded that waterjet is an effective method for piercing short fiber/ceramic composites but the piercing behavior is closely related to the fiber orientation.

Keywords: ceramic-matrix composite, carbon fiber, waterjet, piercing

Kompoziti s keramično matrico in kratkimi vlakni kot ojačitveno fazo so relativno poceni, ker jih je možno izdelovati z enostavnim postopkom. Rezanje oz. mehanska obdelava zelo trdih materialov se pogosto izvaja z vodnim curkom, ki je zelo učinkovit postopek. Vendar pa je bilo do sedaj izvedeno zelo majhno število študij, ki obravnavajo obnašanje vodnega curka med prodiranjem skozi keramične materiale v katerih se nahajajo kratka vlakna. V študiji so avtorji izdelali C_f/Al_2O_3 kompozit z *in-situ* pretvorbo predoksidiranih poliakrilonitrilnih vlaken v ogljikova (C_f) vlakna, med enoosnim vročim sintranjem pod tlakom Al_2O_3 matrice. Pod enoosnim tlakom so se vlakna prednostno orientirala vzporedno z vroče stiskano površino. Za primerjavo z izdelanim kompozitom so izbrali izhodno Al_2O_3 keramiko. Eksperimentalni rezultati so pokazali, da je mehansko obdelana površina z večino paralelnih vlaken, ustrezna. Povprečna globina prodiranja vodnega curka v kompozit je bila približno 1,5-krat večja pri uporabi čistega vodnega curka in 5- do 7-krat večja pri uporabi vodnega curka z dodatkom abrazivnega sredstva, kot pri primerjalni čisti Al_2O_3 keramiki. Mehanizmi erozije prodiranja s čistim vodnim curkom so v keramični matrici imeli značilnosti inter- in trans-granularnega preloma ter drobljenja vlaken. Pri uporabi vodnega curka z dodatkom abrazivnega sredstva je prišlo do mikro-prelomov keramičnih zrn skupaj z vlakni. Pri abrazivnem vodnem curku so bili prednostni erozijski mehanizmi mikro-lomljenje zrn Al_2O_3 in vlaken skupaj s plastično deformacijo in mikrotaljenjem delcev abrazivnega sredstva. Avtorji v članku zaključujejo, da je vodni curek učinkovito sredstvo za mehansko rezanje keramičnih kompozitov, ojačanih s kratkimi vlakni, toda način prodiranja vodnega curka v material je ozko povezan z orientacijo vlaken.

Ključne besede: kompoziti s keramično matrico, ogljikova vlakna, vodni curek, prebadanje

1 INTRODUCTION

The waterjet technology is one of the most powerful cutting processes that can deal with basically all kinds of materials without any limitations.[1,2] The behavior of waterjet-machined ceramics has been reported by numerous research works.[3,4] But only a few research studies focus on the machinability of ceramic-matrix composites machined by waterjet.[5] E. Savrun et al.[6] reported on the feasibility of finishing a SiC whisker/Al_2O_3 composite with an abrasive waterjet. As the machining speed increased, the surface became rougher and plastic deformation turned into the dominant erosion mechanism. G. Hamatani et al.[7] explored the machinability of TiB_2 particulate-reinforced SiC exposed to an abrasive waterjet. The depth of slot decreased as the cutting-head speed increased and a piercing hole with a better cutting edge and minimal damage was produced at a small standoff distance. K. Balamurugan et al.[8,9] explored the abrasive-waterjet cutting performance of $LaPO_4$ doped with Y_2O_3 particles. The repetitive cyclic impact load of hard SiC abrasives and water-cooling effect induced a thermal stress, which weakened the grain boundary and caused the propagation of microcracks. M. Ramulu et al.[10] reported on the abrasive-waterjet machining mechanism of continuous Si-C-O fiber-reinforced β-SiC. The piercing process of a composite could be considered as many micro-crack-initiation and erosion cycles. Erosion

*Corresponding author's e-mail:
iamqiaoxu@163.com (Xu Qiao)

mechanisms are micro-fractures of fiber cloth and SiC. However, to the best of our knowledge, there are very few works dealing with the waterjet machining behavior of ceramics incorporated with short fibers.

Short fiber/ceramic composites with relatively low prices and facile preparation procedures have been widely used. They are a popular alternative to pristine ceramics used in various areas, such as microwave-absorbing materials[11] or aircraft engine parts.[12] An in-situ C_f/Al_2O_3 composite is prepared with a novel technique including sintering of alumina and synchronous in-situ transformation of pre-oxidized poly-acrylonitrile (PAN) precursor fibers into carbon fibers,[13] reducing the synthesis cost and protecting the carbon fibers against damage during the preparation process.

In this work, the piercing behavior and erosion mechanisms of the in-situ C_f/Al_2O_3 exposed to a pure waterjet and abrasive waterjet were investigated. This research helped us improve and extend the usage of the novel composite for different applications, and promote the application of waterjet in the machining of ceramics incorporated with short fibers.

2 EXPERIMENTAL PART

2.1 Materials

The in-situ C_f/Al_2O_3 was fabricated using uni-axial hot-pressed sintering in a vacuum. Raw materials included a 77 φ% α-Al_2O_3 powder (the average grain size of 5.2 μm), 20 φ% PAN fibers (a density of 1.4 g/cm^3 and a length of 3–5 mm) and a 3 φ% CaO-MgO-SiO_2 fluxing agent. All of the raw materials were uniformly mixed, and then the mixture was placed into a graphite mold to be treated with hot-pressed sintering in a vacuum chamber at 1550 °C. During the uni-axial hot-pressed sintering process, the PAN fibers were in-situ transformed into carbon fibers and these were preferably orientated parallel to the hot-pressed surface. As shown in **Figure 1**, on the P surface, 90–95 % of the fibers were parallel to the surface, while on the N surface, most of the fibers (90–95 %) were normal to the surface. A homemade Al_2O_3 ceramic was selected for comparison with the in-situ C_f/Al_2O_3. The Al_2O_3 ceramic was composed of a 97 φ% α-Al_2O_3 powder and a 3 φ% CaO-MgO-SiO_2 fluxing agent and was also prepared with hot-pressed sintering in a vacuum at 1550 °C. All the test materials were cut into cuboids with dimensions of 15 mm × 10 mm × 8 mm.

2.2 Pure waterjet

Experiments were conducted with an in-house developed waterjet system. The pure waterjet was generated by forcing pressurized water through a nozzle with an orifice of 100 μm in diameter. The water-supplied pressure was 207 MPa, providing a stable and continuous waterjet. **Figure 2a** depicts the structure of the pure waterjet used in this work. In the core zone, the axial stagnation pressure remains constant, which is equal to the axial pressure at the exit of the nozzle. In the transition zone, the axial stagnation pressure reduces along the jet axis. With the aim of exploring the piercing behavior of the composite at a low impingement power first, the standoff distance was set to 68 mm. According to Equations (1–2), the waterjet was in the transition zone. The axial stagnation pressure and the diameter of the waterjet before hitting a sample was estimated to be approximately 52 MPa and 0.22–0.33 mm, respectively, according to Equations (3–4).[14,15] The test time was 300 s to ensure that the pierced holes were easy to observe. The relationship between the fiber orientation and

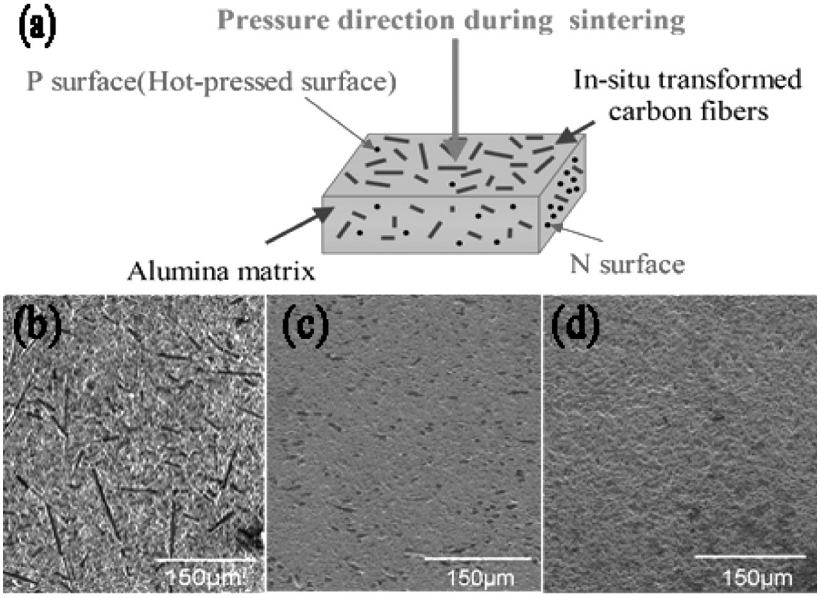

Figure 1: a) Fiber orientation in in-situ C_f/Al_2O_3; microstructures of b) in-situ C_f/Al_2O_3-P, c) in-situ C_f/Al_2O_3-N, d) Al_2O_3

piercing behavior was studied by piercing both the P surface and N surface of the composite. Al_2O_3 was tested under the same condition, as illustrated in **Figure 2b**. Machinability of the materials was evaluated with the piercing depth and material mass loss. Micromorphologies of the pierced holes were observed and analyzed with a HITACHI-3400N and SU8030 field-emission scanning electron microscope (SEM) using Oxford energy-dispersive spectroscopy (EDS).

$$x_c = -3.545\times10^{-11}\times p_0 + 2.535\times10^{-2} \quad (1)$$

$$x_t \approx 5.33 x_c \quad (2)$$

$$p_m = \frac{\varphi^2 p_0 x_c}{x} \quad (x_c < x < x_t, \text{ in transition zone}) \quad (3)$$

$$d = k d_0 \sqrt{\frac{2x}{d_0}}\times10^{-3} \quad (4)$$

Here, x_c is the axial length of the core zone (m); p_0 is the pump pressure (Pa); x_t is the axial length of the transition zone (m); p_m is the axial pressure of the waterjet (Pa); φ is the discharge coefficient, which is measured to be 0.97; x is the standoff distance (m); d is the diameter of the waterjet in the transition zone (mm); k is the coefficient in the range of 0.06–0.09; d_0 is the orifice diameter (mm).

2.3 Abrasive waterjet

Investigation of the piercing behavior of the in-situ C_f/Al_2O_3 machined with pure waterjet clarified the machinability and mechanisms occurring under a low impingement power. To further study the piercing behavior of the composite exposed to an abrasive waterjet, we explored the machining efficiency and erosion mechanisms under a high impingement power.

An abrasive-waterjet cutting system manufactured by Flow, Inc. (model 2b) was employed. The water-supplied pressure was also 207 MPa. **Figure 3a** depicts how an abrasive waterjet is formed. The velocity and power of the abrasive waterjet were roughly 476 m/s and 1807 W, as calculated by Equations (5–6). The viability of drilling the composite with abrasive waterjet was tested on the P surface under high and low impingement energies (energy here is the impingement power multiplied by the test time). Al_2O_3 was also tested under the same condition (**Figure 3b**). Under the high energy, the standoff distance was 18 mm and the test time was 6 s. An extension of the test time would have totally damaged our specimens. Under the low energy, the standoff distance was 40 mm and the test time was 4 s. Although the test time was quite short, the impingement energy of the abrasive waterjet was quite stable. The experimental difference was only about 5 % for the same sample pierced by the abrasive waterjet under the same condition. 80 mesh garnet with a sharp and irregular shape was chosen as the abrasive because it shows the optimum machining ability in most cases.[16,17]

The machinability of the composite was evaluated with piercing depths, top diameters of the piercing holes and material mass losses. An Alicona® Infinite focus microscope was adopted to obtain 3D profiles of the holes. Mass losses of the specimens were acquired with a high-precision electronic balance with an accuracy of 0.0001 g. Micromorphologies of the holes were observed with the SEM and EDS mentioned in Section 2.2.

$$v_c = \frac{v_w}{1+\frac{w_a}{\rho_w Q}} \quad (5)$$

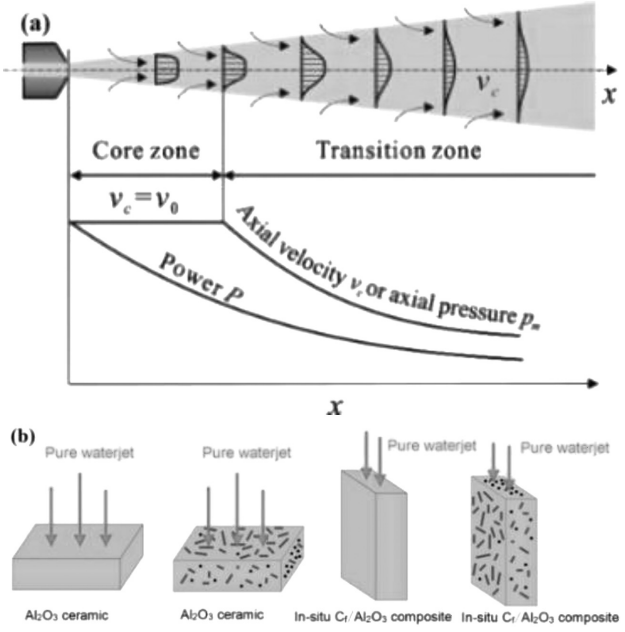

Figure 2: a) Structure of pure waterjet, b) schematic diagrams of piercing experiments with pure waterjet

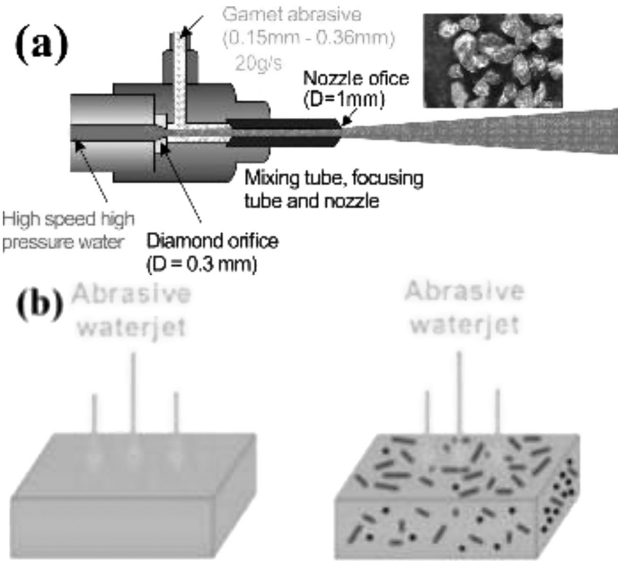

Figure 3: a) schematic diagram of abrasive waterjet, b) piercing experiments using abrasive waterjet

$$P_a = \frac{0.75\left(\frac{w_a}{\rho_w}\right)p}{\left(1+\frac{w_a}{\rho_w Q}\right)^2} \quad (6)$$

Here, v_c is the velocity of the abrasive waterjet (m/s); v_w is the velocity of the waterjet before its mixing with the abrasive (m/s); w_a is the abrasive flow rate (kg/s); ρ_w is the density of water (kg/m^3); Q is the water flow rate (m^3/s); P_a is the power of the abrasive waterjet (W); p is the pump pressure (Pa).

3 RESULTS AND DISCUSSION

3.1 Machinability in the case of pure waterjet

In terms of the piercing depth (**Figure 4a**), the in-situ C_f/Al_2O_3 shows a comparable or larger piercing depth in comparison to Al_2O_3. As for the influence of the fiber orientation, most of the short fibers parallel to the machined surface improve the machining efficiency. The piercing hole of the in-situ C_f/Al_2O_3-P was, on average, deeper than that of the in-situ C_f/Al_2O_3-N, and the difference between them was about 50 μm.

In terms of top diameters of the piercing holes, all of the test materials displayed irregular shapes (**Figure 4a**).

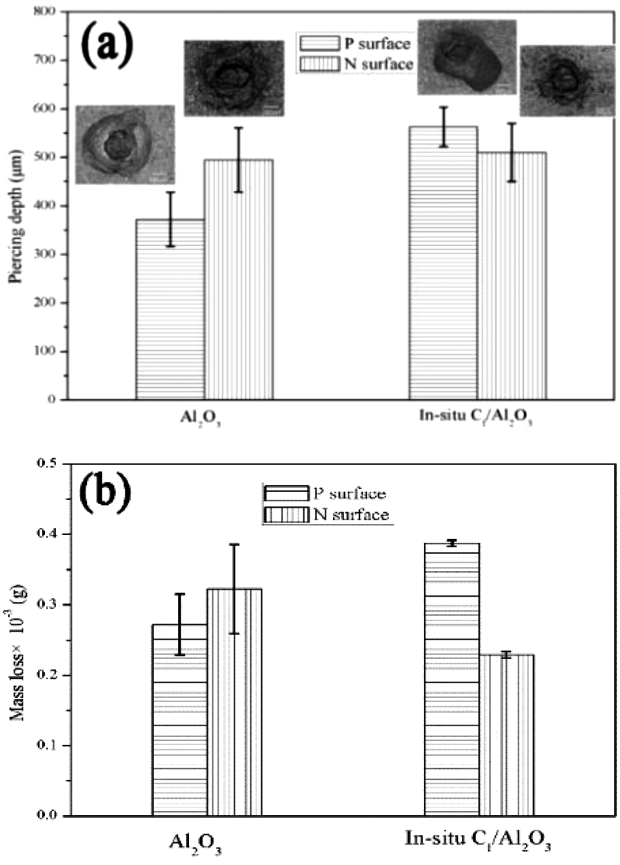

Figure 4: a) piercing depths and b) material mass losses of test materials

Therefore, the evaluation of the piercing rates by comparing the top diameters was not adopted. However, in the Al_2O_3 without the fibers, when it was hit by the waterjet, cracks propagated relatively freely along the grain boundary or through grains. Nevertheless, in the in-situ C_f/Al_2O_3, the propagation of cracks was hampered by the carbon fibers. Consequently, from the top view, the piercing holes of the in-situ C_f/Al_2O_3 are relatively regular and round compared to Al_2O_3.

The other comparative criterion, the material mass loss, exhibits a trend similar to that of the piercing depth. The average mass loss of the in-situ C_f/Al_2O_3-P is the highest among all the test materials (**Figure 4b**). Material losses of Al_2O_3 vary strongly due to its inherent brittleness. The mass losses of the composite are therefore much more stable.

3.2 Erosion mechanisms due to pure waterjet

As a waterjet hits a sample surface, the free end surface of the jet beam is compressed greatly because of a sudden change of the waterjet velocity. The compression of the free jet beam forms a shock energy wave absorbed by samples. A pristine ceramic usually absorbs the external energy by means of crack generation and propagation because its rigid structure leads to a lack of plastic deformation.[18] Cracks are easily formed on weakness planes and grain boundaries. The waterjet beam flows into the cracks and then this fluid "wedge" is pressurized by the arrival of the subsequent slug of water, creating a higher-pressure wedge, which lengthens the existent cracks.[19] The cracks propagate in the radial and vertical directions and come across each other causing material removal. It can be seen in **Figure 5a** that Al_2O_3 pierced by the pure waterjet displays an intergranular or transgranular fracture. As for the composite, the alumina matrix displays similar morphologies with Al_2O_3, namely an intergranular or transgranular fracture. In addition, fiber spalling or pullout are observed (**Figures 5b** to **5c**). Fiber orientation has a significant effect on the machinability and erosion mechanisms. Interfaces between fibers and the alumina matrix are heterogeneous, having a lower strength than that of the alumina grain boundary and intragrain region. For the in-situ C_f/Al_2O_3-P, 90%–95%, fibers are parallel to the surface. When the waterjet penetrates interfaces, fibers are easy to spall so alumina grains around the fibers are relatively easy to be removed, giving rise to a better machinability. On the other hand, for the in-situ C_f/Al_2O_3-N, 90–95 % of the fibers are normal to the surface. When the waterjet penetrates the interfaces, the fibers are hard to spall, inhibiting the crack growth, so the material removal rate is quite low. When alumina grains around the fibers are removed, the fibers are pulled out and removed by the water. The above erosion mechanisms are also illustrated in **Figure 5**. The longer the fiber that is to be pulled out, the more energy is needed. The ratio of the highest fiber-pullout energy to the highest fiber-spalling energy

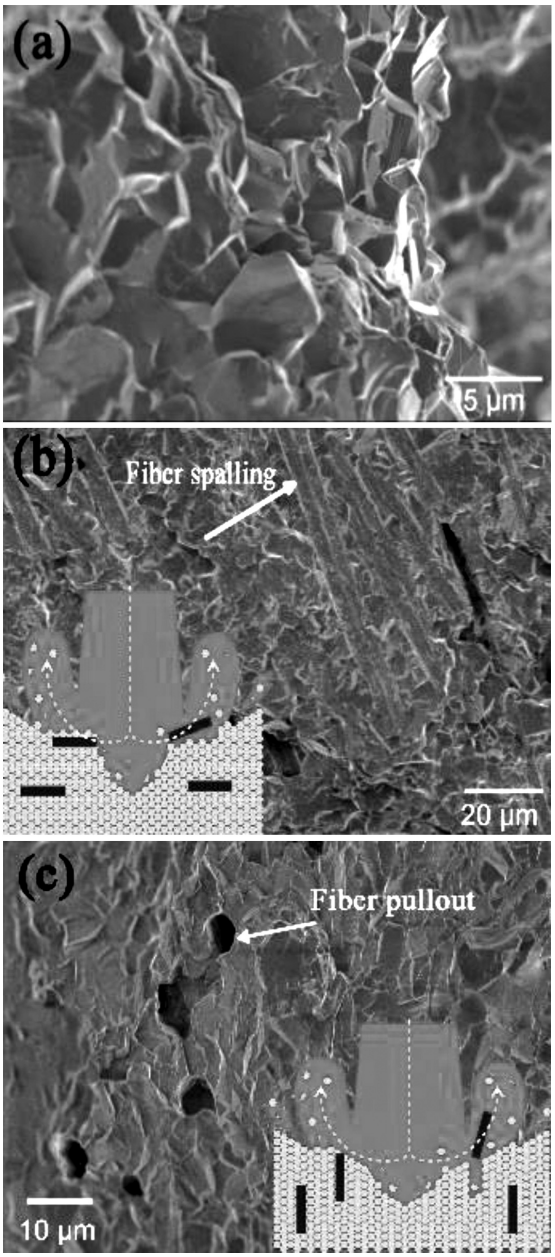

Figure 5: Micromorphologies of: a) Al_2O_3, b) in-situ C_f/Al_2O_3-P and c) in-situ C_f/Al_2O_3-N pierced by pure waterjet

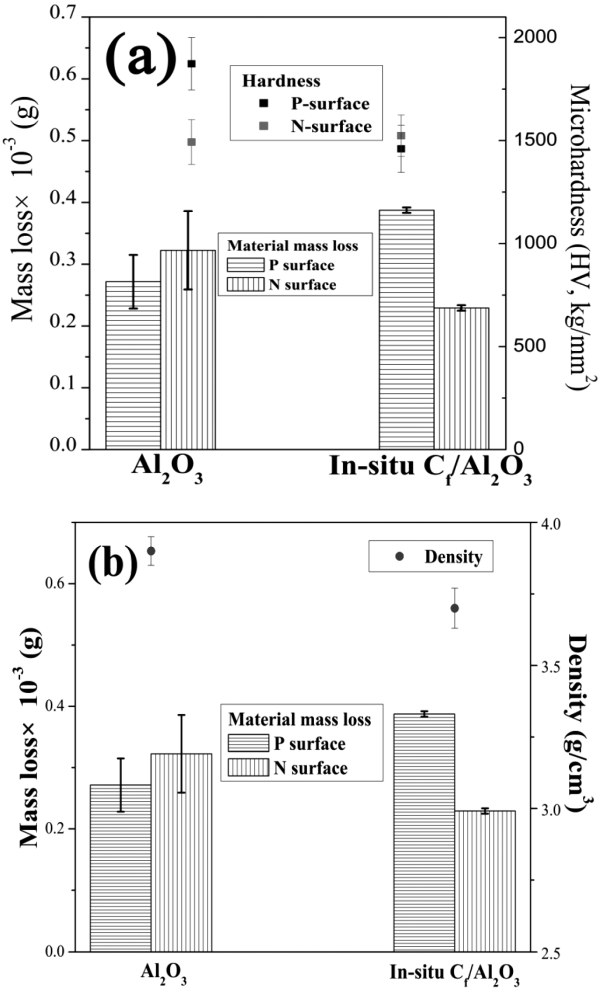

Figure 6: Relationship between material losses and a) microhardness values, b) densities of test materials

is roughly three times the ratio of the elastic modulus to the tensile fracture strength of a fiber,[20] so in this case, the highest fiber-pullout energy is about 180 times the highest fiber-spalling energy. That is to say, the fiber pullout consumes a significantly greater amount of the waterjet energy than the fiber spalling. Therefore, the material mass loss of the in-situ C_f/Al_2O_3-N is the lowest among all the test materials.

The composite has a lower density and hardness value compared with Al_2O_3 because of the carbon-fiber addition. [13] Densities, instead of hardness values, are closely related to the piercing depth of the test materials (**Figure 6**). The in-situ C_f/Al_2O_3-P is easier to be machined than Al_2O_3. However, the machinability of the composite is very sensitive to the fiber orientation: when most of the fibers are normal to the surface, the fiber pullout absorbs plenty of machining energy and weakens the piercing capacity.

3.3 Piercing behavior in the case of abrasive waterjet

When pure waterjet pierces the in-situ C_f/Al_2O_3, the machined surface with most of its fibers being parallel shows a better machinability than the surface with most of its fibers being normal to it. Therefore, during the following experiments with an abrasive waterjet, we only focused on the piercing behavior of the in-situ C_f/Al_2O_3-P and, correspondingly, chose Al_2O_3-P for comparison.

The in-situ C_f/Al_2O_3-P pierced by an abrasive waterjet is super-efficient. Piercing holes of the composite are deeper and narrower than those of the pristine alumina (**Figure 7**). The piercing depth of the composite is around 5–7 times higher than that of Al_2O_3-P. Besides, the piercing depth of the composite grows rapidly with

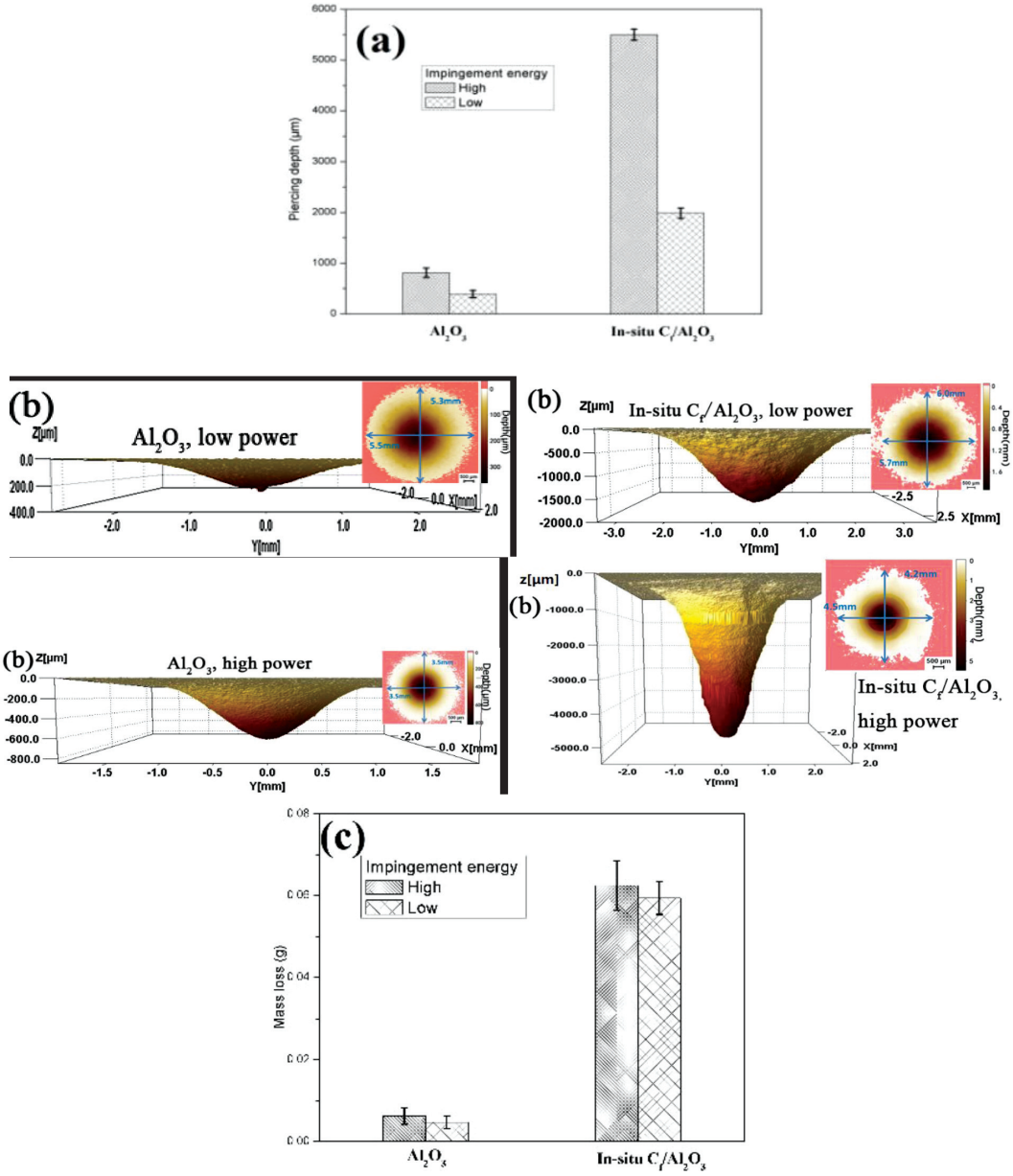

Figure 7: a) Piercing depth, b) three dimensional profiles and c) material mass losses of test materials pierced by abrasive waterjet

an impingement-energy increase in comparison to the pristine ceramic. Moreover, under both high and low impingement energies, the average top diameters of the piercing holes of the composite are smaller than that of the pristine ceramic, being 1.9 mm and 1.5 mm, respectively. With regard to material losses, the composite displays a higher mass loss than the pristine ceramic. The piercing behavior in the abrasive-waterjet machining of the in-situ C_f/Al_2O_3-P is quite satisfactory, especially under the high impingement energy.

3.4. Erosion mechanisms due to abrasive waterjet

Morphologies of the piercing holes of the in-situ C_f/Al_2O_3-P under the high impingement energy are shown, from the top to the bottom, in **Figure 8**. At the top, alumina grains reveal transgranular or intergranular fractures and a plastic grain deformation. However, no fibers are observed. The composite is repetitively impinged by ultra-high-speed abrasives, generating a huge amount of thermal energy. Because alumina has a low thermal conductive coefficient, the localized thermal energy is high enough to soften alumina grains or induce an intergranular slip and thus the alumina matrix displays plastic deformation.[21] The heated zone then suddenly cools down by following the excess water flow, which creates the thermal stress promoting the crack growth.[22] The reason why no fibers or fiber spalling are observed is because fibers detach from the alumina matrix under an impact of an ultra-high-speed abrasive

waterjet and then the alumina grains at the interface are removed easily and quickly or some alumina grains plastically deform, covering spalling spots. In addition, localized micro-melting of abrasives is found in some areas, marked by blue. Abrasives repetitively impact the composite at an ultra-high speed generating a great amount of thermal energy and frictional heat, which produces the melting effect.[22] According to the EDS results, as illustrated in **Figure 8d**, the contents of the Fe and Si elements at the plastic-deformation spots and melting spots are higher than in the alumina matrix. Garnet abrasives are composed of iron oxide and silicon dioxide. This confirms the interaction between the abrasives and alumina. In addition, a few garnet abrasives are found at the bottom of the piercing hole with a diameter of 40–100 μm, while the original size of the abrasives is in a range of 150–360 μm. This also proves the interaction between the abrasives and alumina grains.

Erosion mechanisms in the middle part of the piercing hole are similar to those at the top, as shown in **Figure 8b**. However, at the bottom, erosion mechanisms are different (**Figure 8c**). Plastic deformation and alumina-grain spalling are the dominant mechanisms. Micro-melting of the garnet abrasives is not found. Moreover, it can be seen that some in-situ transformed carbon fibers fracture or spall at the bottom of the piercing hole. When a material is pierced by abrasive waterjet, the energy of water and abrasives is absorbed by the material and it transforms into an internal energy resulting in a material failure. Therefore, the energy of the waterjet dissipates with the piercing depth, resulting in the erosion mechanisms at the top of the hole, which are different from those at the bottom.

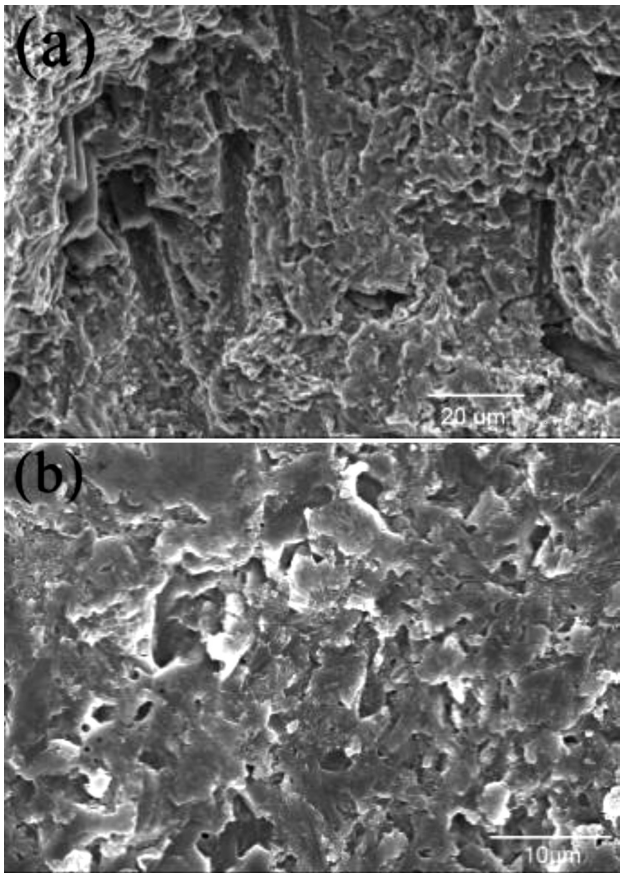

Figure 9: Micromorphologies of: a) in-situ C_f/Al_2O_3-P and b) Al_2O_3 pierced by abrasive waterjet under the low impingement energy

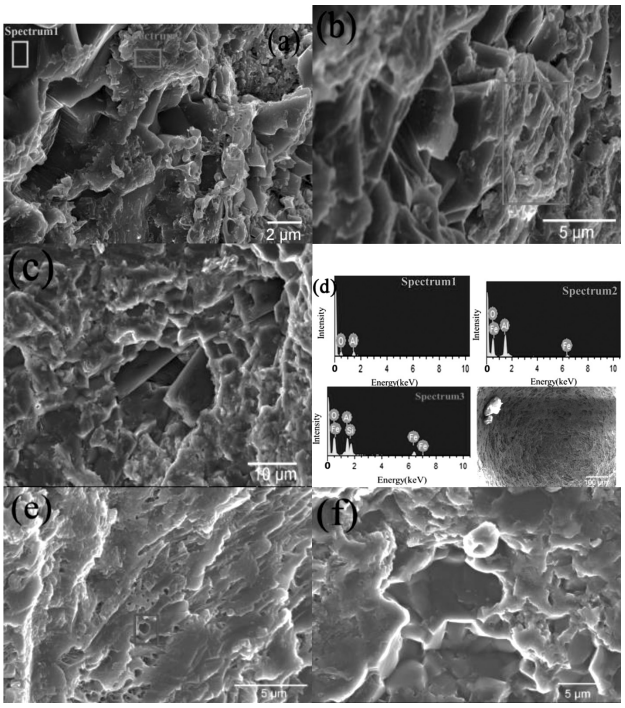

Figure 8: Morphologies of test materials pierced by abrasive waterjet under high impingement power: a) top, b) middle, c) bottom, d) EDS results for in-situ C_f/Al_2O_3-P, e) top, f) bottom of Al_2O_3 (micro-melting is marked by blue)

The micomorphology of Al_2O_3-P under the high impingement energy is similar to that of the matrix of the composite. At the top of the piercing hole, an intergranular or transgranular fracture of alumina grains and micro-melting are observed (**Figure 8e**). At the bottom, deformed alumina grains are surrounded by fractured grains (**Figure 8f**).

Under the low impingement energy, as shown in **Figure 9**, for the composite, a fiber fracture or spalling from the top to the bottom of the hole can be seen, and for the pristine alumina, more alumina grains deform and fewer grains spall. This is associated with the impingement-energy decrease.

4 CONCLUSIONS

1) Waterjet is an effective method for piercing ceramics incorporated with short fibers. The average piercing depth of the in-situ C_f/Al_2O_3-P pierced by a pure waterjet is by approximately 200 μm higher in comparison with Al_2O_3-P. Noticeably, in the case of an abrasive waterjet, the piercing depth of the composite is around 5–7 times higher than that of pristine ceramic.

2) When the in-situ C_f/Al_2O_3 is pierced by a pure waterjet, the alumina matrix shows intergranular and transgranular fractures. In comparison, when the in-situ C_f/Al_2O_3 is pierced by an abrasive waterjet, in addition to alumina grain fractures, a grain plastic deformation and micro-melting of the abrasives are also found.

3) The fiber orientation significantly influences the piercing behavior of the composite. When the pure waterjet pierces the machined surface with most of the fibers being parallel to it, the hole is, on average, 50 μm deeper as compared to the machined surface with its fibers mostly normal to it. This is because the fibers parallel to the machined surface are easy to spall or fracture, promoting the removal of the alumina grains around the fibers. In contrast, when the fibers are normal to the surface, they are hard to spall, inhibiting the crack prorogation, and the fiber pull-out consumes plenty of the machining energy, which weakens the piercing ability.

Acknowledgment

The authors appreciate Yi She (Northwestern University, USA) for his valuable suggestions and assistance, Prof. Wang (Northwestern University, USA) and Prof. Chen (China University of Mining and Technology, Beijing, China) for their guidance.

5 REFERENCES

[1] K. Gupta, Advanced Manufacturing Technologies, Materials Forming, Machining and Tribology: S. Bhowmik, A. Ray, Abrasive water jet machining of composite materials, 2017, 77–97

[2] A. Akkurt, Experimental investigation of the surface properties obtained by cutting brass-353 (alpha+beta) with an abrasive water jet and other cutting methods, Mater. Tehnol., 48 (**2014**), 725–734

[3] S. Saurabh, T. Tiwari, A. Nag, A. Dixit, N. Mandal, A. Das, A. Mandal, A. K. Srivastava, Processing of alumina ceramics by abrasive waterjet – an experimental study, Mater. Today: Proc., 5 (**2018**) 9, 18061–18069, doi:10.1016/j.matpr.2018.06.140

[4] K. Kowsari, H. Nouraei, B. Samareh, M. Papini, J. K. Spelt, CFD-aided prediction of the shape of abrasive slurry jet micro-machined channels in sintered ceramics, Ceram. Int., 42 (**2016**) 6, 7030–7042, doi:10.1016/j.ceramint.2016.01.091

[5] O. G. Diaz, G. G. Luna, Z. Liao, D. Axinte, The new challenges of machining ceramic matrix composites (CMCs): Review of surface integrity, Int. J. Mach. Tool. Manu., 139 (**2019**), 24–36, doi:10.1016/j.ijmachtools.2019.01.003

[6] E. Savrun, M. Taya, Surface characterization of SiC whisker/2124 aluminium and Al_2O_3 composites machined by abrasive water jet, J. Mater. Sci., 23 (**1988**), 1453–1458, doi:10.1007/BF01154616

[7] G. Hamatani, M. Ramulu, Machinability of high temperature composites by abrasive waterjet, J. Eng. Mater.-T. ASME, 112 (**1990**) 4, 381–386, doi:10.1115/1.2903346.

[8] K. Balamurugan, M. Uthayakumar, S. Sankar, U. Hareesh, K. Warrier, Abrasive waterjet cutting of lanthanum phosphate–yttria composite: A comparative approach, Recent Developments, Springer, Cham. 2019, 101–119

[9] K. Balamurugan, M. Uthayakumar, S. Sankar, U. Hareesh, K. Warrier, Predicting correlations in abrasive waterjet cutting parameters of lanthanum phosphate/yttria composite by response surface methodology, Measurement, 131 (**2019**), 309–318, doi:10.1016/j.measurement.2018.09.009

[10] M. Ramulu, M. Jenkins, Z. Guo, Abrasive water jet machining mechanisms in continuous-fiber ceramic composites, J. Composite. Technol. Res., 23 (**2001**), 82–91, doi:10.1520/CTR10916J

[11] S. Huang, W. Zhou, P. Wei, F. Luo, D. Zhu, K. Sun, Short-carbon-fiber reinforced alumina ceramic with improved mechanical property and dielectric property in the Ku-band, Phys. Status. Solidi. A, 210 (**2013**), 1944–1949, doi:10.1002/pssa.201329258

[12] S. Tang, C. Hu, Design, preparation and properties of carbon fiber reinforced ultra-high temperature ceramic composites for aerospace applications: A review, J. Mater. Sci. Technol., 33 (**2017**) 2, 117–130, doi:10.1016/j.jmst.2016.08.004

[13] J. Ren, H. Chen, B. Ma, F. Zhao, C. Wang, H. Hong, Y. Li, X. He, X. Chen, R. An, Tribological performance of in-situ transformed C_f/Al_2O_3 self-lubricating composite, Wear, 376–377 (**2017**), 363–371, doi:10.1016/j.wear.2016.12.020

[14] S. Xue, Y. Jiao, Q. Zhang, Y. Fan, High pressure waterjet technology & engineering, Hefei University of Technology Press, Hefei 2006

[15] R. Wang, Study on rock breaking mechanism under high pressure water jet, China University of Petroleum Press, Dongying 2010

[16] P. Thamizhvalavan, S. Arivazhagan, N. Yuvaraj, B. Ramesh, Machinability study of abrasive aqua jet parameters on hybrid metal matrix composite, Mater. Manuf. Process., 34 (**2019**) 3, 321–344, doi:10.1080/10426914.2018.1544707

[17] H. Li, J. Wang, An experimental study of abrasive waterjet machining of Ti-6Al-4V, Int. J. Adv. Manuf. Technol., 81 (**2015**) 1–4, 361–369, doi:10.1007/s00170-015-7245-5

[18] D. K. Shanmugam, T. Nguyen, J. Wang, A study of delamination on graphite/epoxy composites in abrasive waterjet machining, Compos. Part A-Appl. S., 39 (**2008**) 6, 923–929, doi:10.1016/j.compositesa.2008.04.001

[19] D. A. Summers, Waterjetting technology, Taylor & Francis, New York 1995

[20] H. Chen, H. Deng, M. Li, X. Lin, Modern composite materials, China Fortune Press, Beijing 1998

[21] J. Zeng, T. J. Kim, An erosion model of polycrystalline ceramics in abrasive waterjet cutting, Wear, 193 (**1996**) 2, 207–217, doi:10.1016/0043-1648(95)06721-3

[22] A. W. Momber, R. Kovacevic, Principles of abrasive water jet machining, Springer, London 2012